A *Chandra* ACIS Study of the Young Star Cluster Trumpler 15 in Carina and Correlation with Near-infrared Sources

Junfeng Wang,[1] Eric D. Feigelson,[2] Leisa K. Townsley,[2] Patrick S. Broos,[2] Konstantin V. Getman,[2] Scott J. Wolk,[1] Thomas Preibisch,[3] Keivan G. Stassun,[4,5] Anthony F. J. Moffat,[6] Gordon Garmire,[2] Robert R. King,[7] Mark J. McCaughrean,[7,8] and Hans Zinnecker[9]

ABSTRACT

Using the highest-resolution X-ray observation of the Trumpler 15 star cluster taken by the *Chandra X-ray Observatory*, we estimate the total size of its stellar population by comparing the X-ray luminosity function of the detected sources to a calibrator cluster, and identify for the first time a significant fraction ($\sim$14%) of its individual members. The highest-resolution near-IR observation of Trumpler 15 (taken by the HAWK-I instrument on the VLT) was found to detect most of our X-ray selected sample of cluster members, with a K-excess disk frequency of 3.8 ± 0.7%. The near-IR data, X-ray luminosity function, and published spectral types of the brightest members support a cluster age estimate (5–10 Myr) that is older than those for the nearby Trumpler 14 and Trumpler 16 clusters, and

[1]Harvard-Smithsonian Center for Astrophysics, 60 Garden St, Cambridge, MA 02138

[2]Department of Astronomy & Astrophysics, The Pennsylvania State University, 525 Davey Lab, University Park, PA 16802

[3]Universitäts-Sternwarte München, Ludwig-Maximilians-Universität, Scheinerstr. 1, 81679 München, Germany

[4]Department of Physics & Astronomy, Vanderbilt University, Nashville, TN 37235

[5]Department of Physics, Fisk University, 1000 17th Ave. N., Nashville, TN 37208

[6]Département de Physique, Université de Montréal, Succursale Centre-Ville, Montréal, QC, H3C 3J7, Canada

[7]Astrophysics Group, College of Engineering, Mathematics, and Physical Sciences, University of Exeter, Exeter EX4 4QL, UK

[8]ESA Research and Scientific Support Department, ESTEC, Postbus 299, 2200 AG Noordwijk, The Netherlands

[9]Astrophysikalisches Institut Potsdam, An der Sternwarte 16, 14482 Potsdam, Germany

suggest that high-mass members may have already exploded as supernovae. The morphology of the inner ∼0.7 pc core of the cluster is found to be spherical. However, the outer regions (beyond ∼2 pc) are elongated, forming an "envelope" of stars that, in projection, appears to connect Trumpler 15 to Trumpler 14; this morphology supports the view that these clusters are physically associated. Clear evidence of mass segregation is seen. This study appears in a Special Issue of the ApJS devoted to the *Chandra* Carina Complex Project (CCCP), a 1.42 square degree *Chandra* X-ray survey of the Great Nebula in Carina.

Subject headings: ISM: individual (Great Nebula in Carina) - open clusters and associations: individual (Trumpler 15) - stars: pre-main sequence - X-Rays: stars

1. Introduction

Trumpler 15(=C 1042-591 = Lund 558 = Ocl 825) is a compact and rich young open cluster located near the northeast edge of the Carina Nebula (see Smith & Brooks 2008 for a review). In contrast to other young clusters in the region, such as Trumpler 14 and Trumpler 16, it is poorly studied: only a few optical and near infrared (near-IR) investigations exist in the literature and ∼20 candidate members have spectral classification (Morrell et al. 1988; Skiff 2009), limited to the brightest OB stars.

The optical and near-IR studies are mainly hampered by the heavy contamination from background stars, since there is little dust in the region and no dense molecular cloud behind the cluster (Carraro 2002). The basic properties of the cluster from major studies in the literature since the 1960s are summarized in Table 1. There was considerable disagreement on the distance (e.g., Thé & Vleeming 1971; Walborn 1973) and age of Trumpler 15 until recent studies with modern CCD photometry (e.g., Carraro 2002; Tapia et al. 2003). Consequently, the relationship of Trumpler 15 to the other clusters (e.g., Trumpler 14/16) located closer to the luminous blue variable (LBV) star η Carinae (Davidson & Humphreys 1997) has been unclear. There is strong observational evidence that massive star formation in the Carina Nebula has been active for several million years and is ongoing (Vazquez et al. 1996, Smith et al. 2000, Ascenso et al. 2007). For Trumpler 15, Dias et al. (2002) list a cluster age of 8 Myr, while Tapia et al. (2003) suggest a range of ages between 4 Myr and 30 Myr with a median value of ∼8 Myr. This is consistent with a picture where Trumpler 15 likely resulted from an early burst of star formation in the complex.

Perhaps due to the historically sparse coverage of optical and near-IR studies, there has been no previous X-ray study of this star cluster. High-resolution X-ray images of young

stellar clusters are effective in detecting large populations of pre-main sequence (PMS) stars with little contamination from Galactic field stars (see Feigelson et al. 2007 for a review). X-ray selection is particularly useful because it traces magnetic flaring that is largely insensitive to the presence or absence of a protoplanetary disk. X-ray samples are thus complementary to infrared-excess samples which locate young stars with dusty disks.

In this paper we present a *Chandra* imaging study of Trumpler 15, aiming to obtain the first X-ray census of its member stars. Section 2 gives a brief description of our *Chandra* observation, and presents a list of X-ray selected young stellar members. Using X-ray, optical, and near-IR data we study in Section 3 the cluster morphology, X-ray luminosity function (XLF), extinction, and age. Section 4 presents notes on some interesting stars. Our findings are summarized in Section 5. As in all CCCP papers (Townsley et al. 2011a), we adopt a distance of 2.3 kpc to Trumpler 15 (Smith 2006) throughout the paper; thus, $1'$ on the sky corresponds to 0.7 pc.

2. Observations and Data Analysis

Trumpler 15 was observed as part of the *Chandra Carina Complex Project* (CCCP; PI: L. Townsley), a large mosaic of *Chandra* Advanced CCD Imaging Spectrometer I-array (ACIS-I) observations. Townsley et al. (2011a) provide a complete overview of the CCCP. One CCCP pointing (ObsID 9484, a 60 ks integration obtained on August 19, 2008) is centered on Trumpler 15; five other pointings cover the edges of the cluster (Figure 1a).

Broos et al. (2011a) describe the custom data preparation, source detection, and source extraction (14369 ACIS point sources) procedures[1] applied to the CCCP data; Broos et al. (2011b) present a source classifier for Carina X-ray source membership that calculates probabilities that a given X-ray source is a foreground star, a background star, an extragalactic source, or a Carina member with careful evaluation of the contaminating populations (Getman et al. 2011). We adopt these classifications in this study, recognizing that they are not perfect; some false positives (contaminants incorrectly identified as Carina members) and false negatives (true Carina members unclassified or incorrectly identified as contaminants) are present. X-ray point source fluxes and absorptions have been estimated with a non-parametric method using median X-ray energy and observed photon flux (XPHOT; Getman et al. 2010).

---

[1]Most of the software required to produce the CCCP source catalog is publicly available in the *ACIS Extract* package (http://www.astro.psu.edu/xray/acis/acis_analysis.html) (Broos et al. 2010).

Feigelson et al. (2011) investigated the spatial distribution of the X-ray sources classified as likely Carina members and the clustering structure based on maps of smoothed source surface density. Trumpler 15 is one of the 20 identified principal clusters (CCCP-Cl#8; Figure 1b in Feigelson et al. 2011) obtained by smoothing a spatially complete sample of likely Carina members with a Gaussian kernel ($\sigma = 30''$, corresponding to $FWHM = 0.8$ pc). In this paper, we adopted a footprint for the Trumpler 15 cluster that is slightly larger than region CCCP-Cl#8. The footprint traces the lowest source density contour presented by Feigelson et al. (2011, Figure 1) and a boundary drawn by-eye to separate Trumpler 15 from Trumpler 14 (see Figure 11 in Townsley et al. 2011a for a global view of Carina's historically-recognized constituent clusters).

The adopted Trumpler 15 region contains 841 CCCP sources, listed in Table 2. Detailed source properties can be extracted from the CCCP catalog (Broos et al. 2011a). The stellar sample we discuss henceforth consists of the 829 sources (98.6%) classified as probable Carina members (Broos et al. 2011b), identified by the "H2" class in Table 2. Broos et al. (2011b) estimate that a few percent of the "H2" sources in the rich cluster region may in fact be foreground Galactic field stars or background extragalactic sources.

Counterparts to CCCP sources have been identified in many optical and IR studies (Broos et al. 2011a). The near-IR data used in this study (Section 3.3) were obtained from the deep HAWK-I[2] survey (Preibisch et al. 2011). A total of 748 (89%) of the ACIS sources have near-IR counterparts with valid $JHKs$ photometry in at least one band; 738 (88%) have valid $JHKs$ photometry in all three bands. Details of the HAWK-I photometric quality is described in Preibisch et al. (2011) (and references therein); briefly, most sources with $J \lesssim 21.2$, $H \lesssim 20.3$, and $Ks \lesssim 19.3$ have formal photometric uncertainties < 0.1 mag ($S/N > 10$ detections).

3. X-ray Cluster Properties

3.1. Cluster Morphology

Figures 1 and 2 show the cluster region in three bands. Figure 1a is a wide-area view of the 2MASS survey with the CCCP ACIS fields delineated. The two brightest stars in the field are red supergiants (RSGs), RT Car (M2Iab) and BO Car (M4Iab), at $K \sim 1.5$ mag; no firm conclusion has been drawn about their membership to Trumpler 15 (Tapia et al.

---

[2]The High Accuity Wide-field K-band Imager, an instrument on the ESO 8 m Very Large Telescope (VLT). See Kissler-Patig et al. (2008) for more information on HAWK-I.

2003; Smith 2006). The Trumpler 15 cluster lies in the middle of the figure, identified as a sparse concentration of a dozen 2MASS stars. A much richer cluster is seen in the deeper HAWK-I image (Preibisch et al. 2011). The cluster is comparably populous in the CCCP X-ray image, shown in Figure 1b, analyzed here.

Figure 2 shows a smoothed contour map of the X-ray sources on the optical Digital Sky Survey (DSS) image. Carraro (2002) analyzes deep UBV images and finds that the cluster is compact, with a core radius of $\sim 2'$ (1.3 pc). Tapia et al. (2003) measured a cluster size of $r = 5.3'$ using V-band star counts. However, contamination by foreground and background stars prevents study of the low density outer regions of the cluster, which are readily seen in the X-ray band. The X-ray cluster also appears compact and spherical in the inner $r = 1'$ core, but becomes elongated at larger distances ($\sim 6'$ along the north-south direction vs. $\sim 4'$ east-west), as outlined by the contours of source density (Figure 2) and as seen in the X-ray image (Figure 1b). Beyond $r = 3'$, there is an "envelope" of more dispersed stars extending south-west towards Trumpler 14. The continuous distribution of stars between Trumpler 14 and 15 (Feigelson et al. 2011; Townsley et al. 2011a) strongly indicates that Trumpler 15 indeed is part of the Carina complex rather than the spatial superposition of a more distant cluster (Walborn 1995). Both Trumpler 14 and 15 are dominated by a central core where the brightest massive stars are concentrated, whereas Trumpler 16 is comprised of a number of subclusters with widely dispersed massive stars (Wolk et al. 2011). We also note that Trumpler 14 has a much higher star density in its core than either Trumpler 15 or 16.

The X-ray defined cluster center of Trumpler 15 $(\alpha, \delta)_{\text{J2000}} = (10^h44^m43.^s8, -59°21'42'')$ (Feigelson et al. 2011) is in good agreement with the cluster center measured by optical studies $(\alpha, \delta)_{\text{J2000}} = (10^h44^m43.^s2, -59°21'49'')$ (e.g., Carraro 2002), considering that the optical position is predominantly determined by the locations of bright OB stars. The radial density profile of the X-ray cluster is shown in Figure 3, derived by counting stars in concentric annuli around the X-ray cluster peak density. For comparison, the optical radial profile in Carraro (2002) is also shown. Both are sharply peaked in the inner $r < 1'$ region, but the X-ray source density is 4 times higher than that in the optical. This is mainly due to the effectiveness of the X-ray survey locating the low mass PMS cluster members, many of which are missed in the optical due to crowding and bright sources in the core. While the density profile falls smoothly to 2 stars per arcmin^2 in the optical, the X-ray profile extends to 0.5 stars per arcmin^2 and shows a bump at $r = 1.5'$. This density enhancement likely arises from a clump of stars to the north of the cluster center (indicated with a circle in Figure 4a), causing an elongation of the X-ray stellar density contours towards the north. This clump of stars is not apparent in the optical DSS image (Figure 2).

Figure 4a shows the spatial distribution of the O and B stars (ranging from B9 to O9 in Trumpler 15) from the Catalogue of Stellar Spectral Classifications (Skiff 2009). The X-ray detected massive stars will be further discussed in Section 4. Figure 4a also presents the spatial distribution of the X-ray selected K-band excess stars (Section 3.3) that retain optically thick circumstellar disks. These represent the younger stellar population. They are not concentrated towards the cluster center, but follow the broad envelope of the Trumpler 15 X-ray source distribution, including the extension southward towards Trumpler 14.

Cumulative radial distributions for the massive stars and the CCCP sample with X-ray-detected massive stars removed, shown in Figure 4b, reveal clear mass segregation. For example, the enclosed fractions of massive and CCCP stars are 43% and 17% at $r = 1'$, and are 78% and 46% at $r = 2'$. The probability that the two populations actually have the same radial profile was found to be only 0.4%, via a 2-sample Kolmogorov-Smirnov statistic.

3.2. X-ray Luminosity Function

Although the massive stars in Trumpler 15 were identified by early studies (e.g., Grubissich 1968), investigation of the low-mass population (less massive than 4 $M_\odot$) has been limited by overwhelming contamination from background stars (Tapia et al. 2003), thus the total stellar population in Trumpler 15 is still largely unknown. Feigelson et al. (2005) suggested that the measured XLF in a young stellar cluster can be viewed as the convolution of the Initial Mass Function (IMF) and the mass–luminosity correlation (which is measured in the Chandra Orion Ultradeep Project [COUP] studies; Getman et al. 2005, Preibisch et al. 2005). Using the best-studied Orion Nebula Cluster XLF (COUP XLF) as a calibrator, the XLF of a cluster can be used to probe its IMF and to estimate the total X-ray emitting population. Such a population analysis has been performed in several other studies (Getman et al. 2006; Wang et al. 2007; Broos et al. 2007; Wang et al. 2008, 2010; Winston et al. 2010; Wolk et al. 2010). In a similar XLF analysis performed here, we consider the total band (0.5–8 keV) absorption corrected X-ray luminosity, $L_{t,c}$, estimated by XPHOT (Getman et al. 2010; Section 2).

We consistently detect 15 count sources at any off-axis location in the 60 ks exposure (see Figure 7 in Broos et al. 2011a), which allows us to estimate the detection completeness limit in $L_{t,c}$. Assuming an absorption column density $N_H = 3 \times 10^{21}$ cm^{-2} (corresponding to $A_V \sim 2$ mag, typical for Trumpler 15 stars; Carraro 2002) and a thermal plasma with $kT = 1$ keV (typical for young X-ray emitting low-mass stars; e.g., Preibisch et al. 2005), the corresponding ACIS point source luminosity is $\log L_{t,c} \sim 30.4$ erg s^{-1}, calculated with

the Portable Interactive Multi-Mission Simulator (PIMMS[3]) tool.

Figure 5 shows the XLF for 316 Trumpler 15 sources for which $L_{t,c}$ is available ($L_{t,c}$ cannot be obtained for many faint sources) and membership in the Carina complex is likely (the "H2" classification of Broos et al. 2011a). Overplotted is a template XLF obtained from the COUP unobscured population (839 cool stars, excluding high-mass stars with spectral types earlier than B4; Feigelson et al. 2005). Seven X-ray detected O and B stars in Trumpler 15 (Section 4) were excluded to be consistent with the COUP sample.

Comparing to the COUP XLF, the Trumpler 15 XLF turns over quickly at $\log L_{t,c} < 30.4$ due to incompleteness. We model the XLF ($L_{t,c}$) with a power-law distribution, restricted to a range of luminosities above this completeness limit. Parameters of the power-law are derived by directly fitting the luminosity values, without binning, to the model as described by Maschberger & Kroupa (2009). Our choice for the range of luminosities fit was informed by the so-called "stablilized P-P plot" produced by the fitting process (Maschberger & Kroupa 2009; Michael 1983).[4] The slope of the Trumpler 15 XLF ($\Gamma = -0.96 \pm 0.13$) is largely consistent with that of the COUP XLF ($\Gamma = -0.89 \pm 0.07$) in the luminosity range $30.4 \lesssim \log L_{t,c} \lesssim 31.0$ (erg s^{-1}). The 1-σ errors on the power-law slopes were derived using the non-parametric bootstrap method. Matching the two cluster XLFs in the range of $30.4 \lesssim \log L_{t,c} \lesssim 31.0$ requires scaling up the ONC population by a factor of 2.1 ± 0.3. If we assume the ONC has ~ 2800 stars (within a projected 2 pc radius, Hillenbrand & Hartmann 1998), then Trumpler 15 is inferred to have ~ 5900 stars. Note that this is only an approximate measure of the cluster population, as quantitative comparison between Trumpler 15 and the ONC depends on accurate knowledge of their respective distances, physical extents, and absorption characteristics.

However, if the more luminous bins ($\log L_{t,c} \gtrsim 31$) are included in the fit, the slope of the Trumpler 15 XLF becomes much steeper ($\Gamma = -1.27 \pm 0.10$) than the COUP XLF (Figure 5). This cannot be an artifact of the detection completeness limit. The luminosity bins causing the steep slope in the Trumpler 15 XLF are at the brighter end of the XLF, therefore these sources are not missed due to sensitivity. We further consider the small differences between the X-ray detection efficiencies for K_s-excess and non K_s-excess stars (Flaccomio et al 2003, Preibisch et al 2005, Getman et al. 2009, Winston et al. 2010), and for lightly and heavily obscured stars (Feigelson et al 2005). We have explored the XLFs with a smaller Trumpler 15 sample (307 stars) that excludes the K_s-excess stars, and with another sample (262 stars)

---

[3]Available at http://heasarc.nasa.gov/docs/software/tools/pimms.html

[4]The TARA package (http://www.astro.psu.edu/xray/docs/TARA/) provides a tool, *ml_powerlaw*, that implements this bin-free fitting procedure and the stabilized P-P plot.

that excludes the sources with median photon energy $MedE \geq 2.0$ keV; both alternative samples show little impact on the slope of the Trumpler 15 XLF when high luminosity bins are included ($\Gamma = -1.3 \pm 0.1$).

Two mechanisms intrinsic to the Trumpler 15 cluster may be responsible for the observed slope anomaly. First, if Trumpler 15's formation process was consistent with a standard IMF (e.g., Kroupa 2001), then the steep slope may be related to its age. The apparent absence of stars earlier than O9 at the current epoch strongly suggests that massive stars have been lost, presumably by evolving into supernovae (SNe). Specifically, a cluster with 5900 stars is expected to have an average number of 11.5 stars with $M > 20M_\odot$ assuming the Kroupa (2001) IMF. The probability of forming no such massive stars in Trumpler 15 is $< 10^{-5}$, based on 10^6 random realizations of a simulated cluster containing 5900 stars with masses distributed according to the Kroupa (2001) IMF. The notion that the cluster's massive stars (which would be luminous X-ray sources) have been destroyed is consistent with the cluster age estimate (5–10 Myr, Section 3.3) and is supported by the presence of the O9III stars in the cluster, which are possibly the post-main sequence members that will soon evolve to supernovae explosions. In addition, Povich et al. (2011) found some evidence in the CCCP sample that intermediate mass (2–10 $M_\odot$) stars are intrinsic X-ray emitters during their PMS evolution, but then the emission diminishes in a few Myrs or less. Since Trumpler 15 is significantly older than the ONC, our X-ray sample likely misses some intermediate mass stars due to this evolution, which can also contribute to a steeper slope in the observed XLF.

Alternatively, the steep XLF slope may indicate that the Trumpler 15 IMF deviates from the Orion IMF with an excess of ~ 120 stars in the luminosity range $30.4 \lesssim \log L_{t,c} \lesssim 31.0$ erg s^{-1} or, equivalently, deficit of massive stars producing $\log L_{t,c} \gtrsim 31.0$ erg s^{-1}. Although we cannot exclude an anomalous IMF, these extra stars are unlikely to be foreground contaminants that are erroneously classified as Carina members because essentially no stars are found close to the unreddened main sequence locus in the NIR color-magnitude diagram of Trumpler 15 (see next section). To test whether the adjacent Trumpler 14 cluster may contribute additional stars to Trumpler 15, we inspected the spatial distribution of sources that have luminosities in the excess bins; no concentration towards Trumpler 14 was found.

Coincidentally, Carraro (2002) noted an apparent gap in the optical color-magnitude diagram of Trumpler 15, similar to gaps observed for some other open star clusters (e.g., Rachford & Canterna 2000; Kumar et al. 2008). If the gap indeed indicates missing stars with inferred main-sequence spectral type B1–B5 ($7 - 9M_\odot$; Girardi et al. 2000), this anomaly could contribute to the observed deficit in the XLF. However, the origin of these optical color-magnitude gaps is not yet clear: alternative explanations include the abrupt onset of convection in the stellar envelopes (Bohm-Vitense & Canterna 1974) and peculiarities in the

Balmer lines (Mermilliod 1976).

3.3. Near-IR Color-Color and Color-Magnitude Diagrams

We study the near-IR characteristics of Trumpler 15 stars using the sub-sample of 738 X-ray selected sources that have valid $JHKs$ HAWK-I photometry in all three bands. Figure 6 shows the near-IR $J - H$ vs. $H - K$ color-color diagram. The colors of most *Chandra* sources (concentrated at J-H=0.8, H-K=0.3) are consistent with diskless young stars subjected to $A_V \sim 1 - 2$ mag (assuming late type stars).

Following the same K-excess definition as Preibisch et al. (2011)(> 0.05 mag to the right and below the reddened main sequence locus), our sample contains 28 K-band excess stars, yielding a near-IR excess fraction of $3.8 \pm 0.7\%$ in Trumpler 15. The error on the K-excess fraction is calculated using 1-σ Poisson errors on the number of stars. This is slightly higher than the fraction $(2.1 \pm 0.7\%)$ presented in (Preibisch et al. 2011), which used a different stellar sample (436 sources in the CCCP-Cl#8 cluster that have near-IR photometry). Both estimates indicate that the Trumpler 15 excess fraction is lower than in Trumpler 16 and Trumpler 14 which are $6.9 \pm 1.3\%$ and $9.7 \pm 1.6\%$ (Preibisch et al. 2011), respectively. Wolk et al. (2011) found a range of K-excess disk fractions among the Trumpler 16 subclusters (e.g., $4 \pm 3\%$ in subcluster 9 and $18 \pm 4\%$ in the South Extension).

Figure 7 shows the near-IR J vs. $J - H$ color-magnitude diagram (CMD) for the same stars shown in Figure 6. Known OB stars are located at the top, reddened from the ZAMS with $A_V \sim 1$ mag. The X-ray observations do not identify any previously unknown $J < 10$ members of the cluster; the same result was found for other unobscured clusters that are well studied in the optical (e.g., NGC 2244; Wang et al. 2008). The deficit of stars in the range $10 < J < 12$ seen in the diagram is attributed to the known lack of X-ray emission from intermediate mass stars (e.g., Stelzer et al. 2006).

The brightest stars ($J < 14$) in the upper part of Figure 7 are bracketed by the 2 Myr (black line) and the 10 Myr (cyan line) isochrones. An age of 5-10 Myr for the low-mass stars is inferred assuming the visual extinction $A_V \sim 1 - 2$ mag, similar to the findings in Preibisch et al. (2011). While Carraro (2002) suggested a cluster age between 2 Myr and 6 Myr for Trumpler 15, Tapia et al. (2003) found that it is not possible to fit the optical CMD of Trumpler 15 using a single age; a range of ages between 4 Myr and 30 Myr is required. All these studies indicate that Trumpler 15 is more evolved than Trumpler 14 (1–2 Myr; Vazquez 1996) and Trumpler 16 (3–4 Myr; Preibisch et al. 2011), a finding consistent with the lower near-IR excess fraction discussed above.

Note that the spectral type of HD 93249 (O9III), the current most massive member in Trumpler 15, also indicates that its stellar population is likely more evolved than the other two clusters. Although the lifetimes of massive stars are difficult to calculate (and depend on parameters such as rotation, metallicity, and binarity that cannot be known for exploded stars), recent stellar evolution models indicate that stars more massive than 40 $M_\odot$ will produce SNe within 5 Myr (Hirschi et al. 2004). For 20 $M_\odot$ stars, it takes less than 10 Myr. Given Trumpler 15's rich population (Section 3.2), there probably were stars formed with sufficient mass ($\sim 20 - 30 M_\odot$) to become Wolf-Rayet (WR) stars, after passing through a blue supergiant (BSG) and either LBV or maybe RSG phase (see Crowther 2007 for a review). The lack of WR stars in Trumpler 15 at the current epoch (Smith 2006) and the inferred age from the near-IR CMD suggest that the more massive stars have evolved through the WR stage to SN. Although earlier studies did not find much evidence for a recent SN in the Carina complex (Smith & Brooks 2008; Ezoe et al. 2009; Townsley et al. 2011b), the CCCP provides several lines of evidence in favor of SNe from an older generation of stars: a young X-ray-emitting neutron star (Hamaguchi et al. 2009), strong metal-enriched X-ray plasma (Townsley et al. 2011b), and a widely dispersed population of both PMS and OB stars (Feigelson et al. 2011). It is also interesting to note that there are one BSG (Trumpler 15 18) and two RSGs (RT Car and BO Car) in the Trumpler 15 field, which could be evolved massive members. Currently their membership to Trumpler 15 is inconclusive (Morrell et al. 1988; Tapia et al. 2003; Smith 2006).

4. X-rays from Individual Stars

Seven X-ray sources in Trumpler 15, listed in Table 3, are identified as counterparts (Broos et al. 2011b) to stars with OB spectral types (Morrell et al. 1988; Carraro 2002; Skiff 2009). More comprehensive investigations of massive stars are available in CCCP studies by Gagné et al. (2011) and by Nazé et al. (2011).

The visually bright star ($V = 8.4$) HD 93249 (=Cl Trumpler 15 1=CD-58°3536) in the center of Trumpler 15 has the earliest spectral type, O9 III (Morrell 1988; Walborn 1973; but see also Feinstein et al. 1980 who assigned a spectral type O8 II,m). The spectrum (184 X-ray counts) extracted from this source (Figure 8) is well fit ($\chi^2_\nu = 0.9$) using XSPEC (version 12.6, Arnaud 1996) with a $kT = 0.36^{+0.20}_{-0.10}$ keV thermal plasma model (APEC; Smith et al. 2001) absorbed by $N_H = 4.8 \pm 2.5 \times 10^{21}$ cm^{-2} (*tbabs*; Wilms et al. 2000). The elemental abundances were fixed at $Z = 0.3 Z_\odot$ for the spectral fit. This choice of subsolar abundances follows the COUP study of Orion OB stars (Stelzer et al. 2005). The derived X-ray absorption gives an $A_V = 3 \pm 1$ mag (assuming $N_H/A_V = 1.6 \times 10^{21}$ cm^{-2}; Vuong et

al. 2003), consistent with the average optical extinction towards Trumpler 15 ($A_V \approx 2$ mag; Carraro 2002). The absorption corrected total band (0.5-8 keV) X-ray luminosity, $L_{t,c}$, is 7.4×10^{31} erg s^{-1}. Adopting $\log(L_{bol}/L_\odot) = 5.28$ for this spectral type (see Table 4 in Smith 2006), we find $L_x/L_{bol} = 1.0 \times 10^{-7}$, which nicely follows the standard empirical relation (e.g., Seward & Chlebowski 1982; Sana et al. 2006). This star has a low-temperature X-ray plasma consistent with the standard model of shocks within an unstable radiatively driven wind (Lucy & White 1980).

We detect a weak X-ray source (17 counts) $7''$ north of HD 93249, consistent with the position reported for its companion CD-58°3536B (=Cl Trumpler 15 2; O9-9.5 III,nn; Morrell 1988); no analysis of its spectrum was attempted.

Among the census of O stars in Trumpler 15 (Carraro 2002; Smith 2006), we do not detect X-ray emission from two early-type stars: HD 93342 (O9 III), listed as an uncertain member by Feinstein et al. (1980), and a BSG Trumpler 15 18 (O9 I; Morrell et al. 1988). The latter suffers an additional $A_V = 3$ mag of dust extinction compared to the other cluster members (Tapia et al. 2003). If we assume a soft thermal spectrum with temperature of $kT \sim 0.4$ keV as in HD 93249, an absorption column $N_H \sim 10^{22}$ cm^{-2}, and an X-ray luminosity of $L_x \sim 1.5 \times 10^{32}$ erg s^{-1} based on the $\log L_x/L_{bol} \approx -7$ relation, then we predict about ~ 80 counts in the CCCP data from Trumpler 15 18. Therefore the non-detection[5] of this star with an upper limit of a few counts supports a note made in Morrell et al. (1988) that it is probably an evolved background star. A similar calculation applies for HD 93342. Thus, the X-ray evidence suggests that neither HD 93342 nor Trumpler 15 18 are massive Carina members, unless they are obscured by high absorption columns.

Another X-ray star ,CCCP #7584 (CXOGNC J104446.54-592154.0), is worth noting, although it is detected with only 7 net counts. The near-IR counterpart is Cl Trumpler 15 10 (B2V), showing significant K-band excess ($J - H = -0.14$ and $H - K = 0.4$ in Figure 6). It is also identified as a young stellar object showing mid-IR excess emission (source #670; Povich et al. 2011). This high mass star may still possess an optically thick inner accretion disk and belong to the class of Herbig Be stars (Herbig 1960).

---

[5]The full ACIS Extract (Broos et al. 2010) procedure used in the CCCP estimates the probability *ProbNoSrc* that the source counts were due to fluctuations in the observed local background in three bands (soft [0.5–2 keV], hard [2–8 keV], and total [0.5–8 keV]), taking into account the variation of *Chandra* point spread function with off-axis angle and the presence of nearby X-ray point sources. A detection requires both the total source counts $SrcCounts\_t \geq 3$ and the smallest *ProbNoSrc* in the three band < 0.01. See Broos et al.(2011a) for details of CCCP source detection.

5. Summary

The *Chandra* ACIS observations of the Trumpler 15 cluster are presented in the framework of the CCCP survey. The results are summarized as follows:

1. We provide an X-ray source list of the Trumpler 15 region, containing 829 probable Carina members with an X-ray luminosity completeness limit $\log L_{t,c} \sim 30.4$ erg s^{-1}. Positional coincidence matching yields a total of 748 HAWK-I near-IR counterparts. This represents an increase in membership by a factor > 30 over previous optical studies that were mostly limited to OB stars.

2. The X-ray detected population provides the first deep probe of the rich low mass population in this cluster. The projected density of Trumpler 15 stars indicates a compact and spherical structure within the inner $1'$ (0.7 pc) region, and an elongation along the N-S direction at larger distances ($> 4'$) from the core. A continuous "envelope" of dispersed stars connects Trumpler 15 with Trumpler 14 to the SW, affirming the view that the two clusters lie at the same distance. The radial density profile of the X-ray cluster is sharply peaked in the inner $r < 1'$ region, and the massive stars are spatially concentrated towards the cluster center. In contrast, the PMS stars with dusty disks, identified by near-IR excess, are distributed throughout the cluster.

3. We interpret the XLF ($L_{t,c}$) for our Trumpler 15 sources as a standard XLF shape (defined by the COUP ONC) that is incompletely detected for $\log L_{t,c} \lesssim 30.4$ erg s^{-1} and that exhibits a deficit of sources for $\log L_{t,c} \gtrsim 31.0$ erg s^{-1}. This deficit of luminous X-ray sources in the current epoch is best explained by the destruction of massive stars in the original population as they evolved into supernovae. Comparison of the two XLFs within a restricted luminosity range where they have similar slopes indicates that Trumpler 15 has $\sim$5900 stars (2.1 ± 0.3 times the ONC population).

4. The near-IR color-magnitude diagram of X-ray selected sources indicates an age of 5–10 Myr and a K-excess disk frequency of $3.8 \pm 0.7\%$ for the PMS population. This age estimate, the absence of WR stars and main sequence members earlier than O9, and the unusual diffuse X-ray emission in the Carina complex all suggest that the most massive original members of the cluster ($> 20 - 40$ M$_\odot$) have evolved into supernovae.

5. We detected seven massive stars with spectral types ranging from B2 to O9. HD 93249 (O9 III) has the soft spectrum expected for X-ray emission via wind shocks in a massive star. Its X-ray luminosity ($L_{t,c} = 7.4 \times 10^{31}$ erg s^{-1}) is also consistent with the long-standing $\log(L_x/L_{bol}) \sim -7$ relation for O stars. The X-ray source Cl Trumpler 15 10 (B2) is proposed as a candidate Herbig Be star due to its significant K-band excess.

Facilities: CXO (ACIS)

REFERENCES

Arnaud, K. A. 1996, Astronomical Data Analysis Software and Systems V, 101, 17

Ascenso, J., Alves, J., Vicente, S., & Lago, M. T. V. T. 2007, A&A, 476, 199

Bessell, M. S., & Brett, J. M. 1988, PASP, 100, 1134

Bohm-Vitense, E., & Canterna, R. 1974, ApJ, 194, 629

Broos, P. S., Feigelson, E. D., Townsley, L. K., Getman, K. V., Wang, J., Garmire, G. P., Jiang, Z., & Tsuboi, Y. 2007, ApJS, 169, 353

Broos, P. S., Townsley, L. K., Feigelson, E. D., Getman, K. V., Bauer, F. E., & Garmire, G. P. 2010, ApJ, 714, 1582

Broos, P. S., et al. 2011a, ApJS, submitted (CCCP Catalog Paper)

Broos, P. S., et al. 2011b, ApJS, submitted (CCCP Classifier Paper)

Carraro, G. 2002, MNRAS, 331, 785

Crowther, P. A. 2007, ARA&A, 45, 177

Davidson, K., & Humphreys, R. M. 1997, ARA&A, 35, 1

Dias, W. S., Alessi, B. S., Moitinho, A., & Lépine, J. R. D. 2002, A&A, 389, 871

Ezoe, Y., Hamaguchi, K., Gruendl, R. A., Chu, Y.-H., Petre, R., & Corcoran, M. F. 2009, PASJ, 61, 123

Feinstein, A., Moffat, A. F. J., & Fitzgerald, M. P. 1980, AJ, 85, 708

Feigelson, E. D., et al. 2005, ApJS, 160, 379

Feigelson, E., Townsley, L., Güdel, M., & Stassun, K. 2007, in Protostars and Planets V, Eds., B. Reipurth, D. Jewitt, and K. Keil, University of Arizona Press, Tucson, 313

Feigelson, E. D., et al. 2011, ApJS, submitted (CCCP Clustering Paper)

Flaccomio, E., Micela, G., & Sciortino, S. 2003, A&A, 402, 277

Gagné, M., et al. 2011, ApJS, submitted (CCCP Massive Star Signatures Paper)

Getman, K. V., Feigelson, E. D., Townsley, L., Broos, P., Garmire, G., & Tsujimoto, M. 2006, ApJS, 163, 306

Getman, K. V., Feigelson, E. D., Luhman, K. L., Sicilia-Aguilar, A., Wang, J., & Garmire, G. P. 2009, ApJ, 699, 1454

Getman, K. V., Feigelson, E. D., Broos, P. S., Townsley, L. K., & Garmire, G. P. 2010, ApJ, 708, 1760

Getman, K. V., et al. 2011, ApJS, submitted (CCCP Contaminants Paper)

Girardi, L., Bressan, A., Bertelli, G., & Chiosi, C. 2000, A&AS, 141, 371

Grubissich, C. 1968, Zeitschrift fur Astrophysik, 68, 173

Hamaguchi, K., et al. 2009, ApJ, 695, L4

Hillenbrand, L. A., & Hartmann, L. W. 1998, ApJ, 492, 540

Hirschi, R., Meynet, G., & Maeder, A. 2004, A&A, 425, 649

Kissler-Patig, M., et al. 2008, A&A, 491, 941

Kroupa, P. 2001, MNRAS, 322, 231

Kumar, B., Sagar, R., & Melnick, J. 2008, MNRAS, 386, 1380

Lucy, L. B., & White, R. L. 1980, ApJ, 241, 300

Maschberger, T., & Kroupa, P. 2009, MNRAS, 395, 931

Mermilliod, J.-C. 1976, A&A, 53, 289

Meyer, M. R., Calvet, N., & Hillenbrand, L. A. 1997, AJ, 114, 288

Michael J.R., 1983, Biometrika, 70, 1, pp.11-17

Morrell, N., Garcia, B., & Levato, H. 1988, PASP, 100, 1431

Nazé, Y., et al. 2011, ApJS, submitted (CCCP Massive Star Lx/Lbol Paper)

Povich, M. S., et al. 2011, ApJS, submitted (CCCP IR YSOs Paper)

Preibisch, T., et al. 2005, ApJS, 160, 401

Preibisch, T., et al. 2011, ApJS, submitted (CCCP HAWK-I Paper)

Rachford, B. L., & Canterna, R. 2000, AJ, 119, 1296

Sana, H., Rauw, G., Nazé, Y., Gosset, E., & Vreux, J.-M. 2006, MNRAS, 372, 661

Siess, L., Dufour, E., & Forestini, M. 2000, A&A, 358, 593

Seward, F. D., & Chlebowski, T. 1982, ApJ, 256, 530

Stelzer, B., Flaccomio, E., Montmerle, T., Micela, G., Sciortino, S., Favata, F., Preibisch, T., & Feigelson, E. D. 2005, ApJS, 160, 557

Stelzer, B., Micela, G., Hamaguchi, K., & Schmitt, J. H. M. M. 2006, A&A, 457, 223

Skiff, B. A. 2009, VizieR Online Data Catalog, 1, 2023

Smith, N., Egan, M. P., Carey, S., Price, S. D., Morse, J. A., & Price, P. A. 2000, ApJ, 532, L145

Smith, R. K., Brickhouse, N. S., Liedahl, D. A., & Raymond, J. C. 2001, ApJ, 556, L91

Smith, N. 2006, MNRAS, 367, 763

Smith, N., & Brooks, K. J. 2008, Handbook of Star Forming Regions, Volume II, 138

Tapia, M., Roth, M., Marraco, H., & Ruiz, M. T. 1988, MNRAS, 232, 661

Tapia, M., Roth, M., Vázquez, R. A., & Feinstein, A. 2003, MNRAS, 339, 44

Townsley, L. K., et al. 2011a, ApJS, submitted (CCCP Intro Paper)

Townsley, L. K., et al. 2011b, ApJS, submitted (CCCP Diffuse Paper)

Thé, P. S., & Vleeming, G. 1971, A&A, 14, 120

Thé, P. S., Bakker, R., & Antalova, A. 1980, A&AS, 41, 93

Vazquez, R. A., Baume, G., Feinstein, A., & Prado, P. 1996, A&AS, 116, 75

Vuong, M. H., Montmerle, T., Grosso, N., Feigelson, E. D., Verstraete, L., & Ozawa, H. 2003, A&A, 408, 581

Walborn, N. R. 1973, ApJ, 179, 517

Walborn, N. R. 1995, Rev. Mex. Astro. Astrofis. Conf. Ser., 2, 51

Wang, J., Townsley, L. K., Feigelson, E. D., Getman, K. V., Broos, P. S., Garmire, G. P., & Tsujimoto, M. 2007, ApJS, 168, 100

Wang, J., Townsley, L. K., Feigelson, E. D., Broos, P. S., Getman, K. V., Román-Zúñiga, C. G., & Lada, E. 2008, ApJ, 675, 464

Wang, J., Feigelson, E. D., Townsley, L. K., Broos, P. S., Román-Zúñiga, C. G., Lada, E., & Garmire, G. 2010, ApJ, 716, 474

Wilms, J., Allen, A., & McCray, R. 2000, ApJ, 542, 914

Winston, E., et al. 2010, AJ, 140, 266

Wolk, S. J., Winston, E., Bourke, T. L., Gutermuth, R., Megeath, S. T., Spitzbart, B. D., & Osten, R. 2010, ApJ, 715, 671

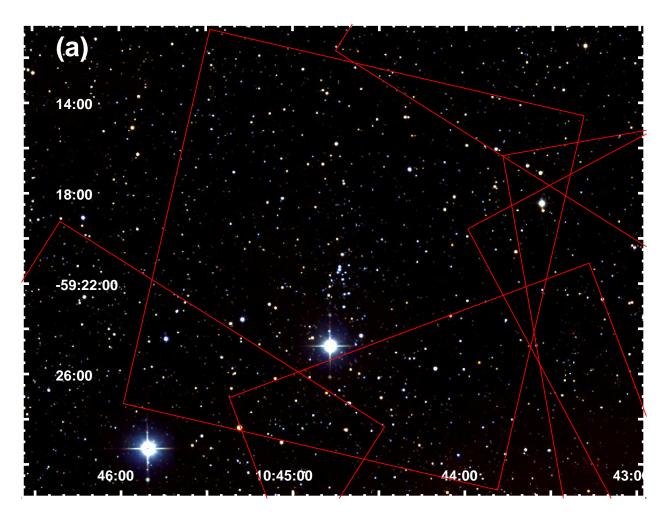Wolk, S. J., et al. 2011, ApJS, submitted (CCCP Tr16 Paper)

Fig. 1.— (a) 2MASS JHK_s composite image of the Trumpler 15 region overlaid with boxes depicting the $17' \times 17'$ ACIS-I fields of view for the CCCP observations.
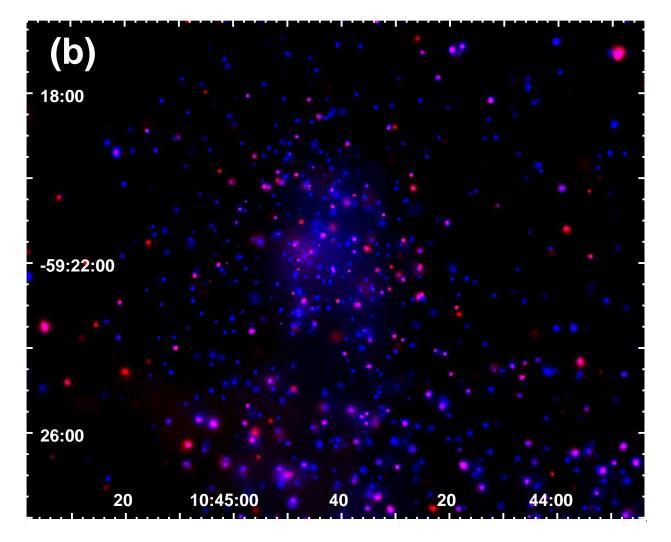
Fig. 1.— (b) Adaptively smoothed *Chandra* ACIS images of Trumpler 15 ($\sim 12' \times 12'$). Red represents the soft-band (0.5–2 keV) X-ray emission and blue the hard X-ray emission (2–7 keV). The sky coordinates are for the epoch J2000 in both panels.
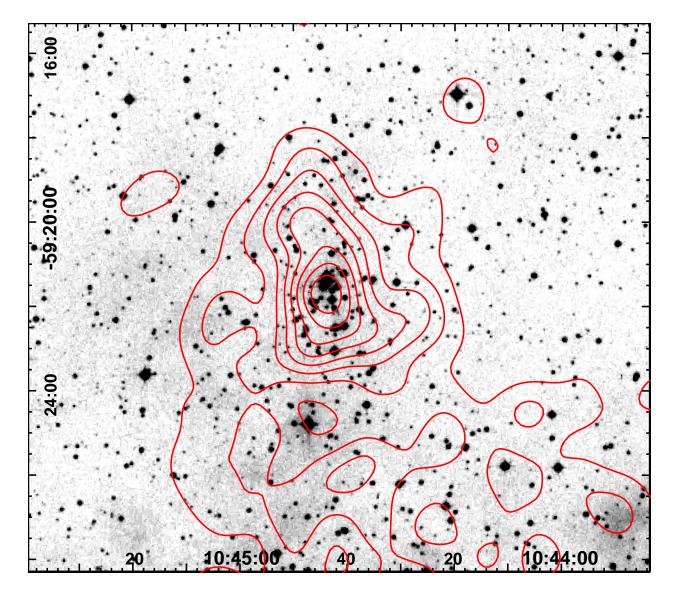
Fig. 2.— DSS *R*-band image of the Trumpler 15 region overlaid with X-ray source density contours (Feigelson et al. 2011). The sky coordinates are for the epoch J2000.
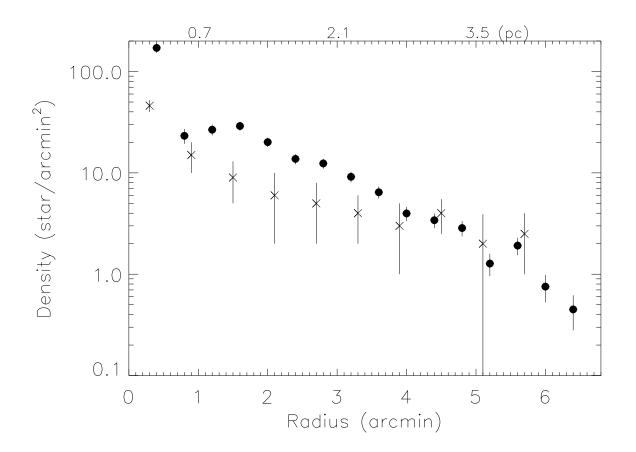
Fig. 3.— Radial density profile of X-ray sources (filled circles) and optical sources (crosses, Carraro 2002).
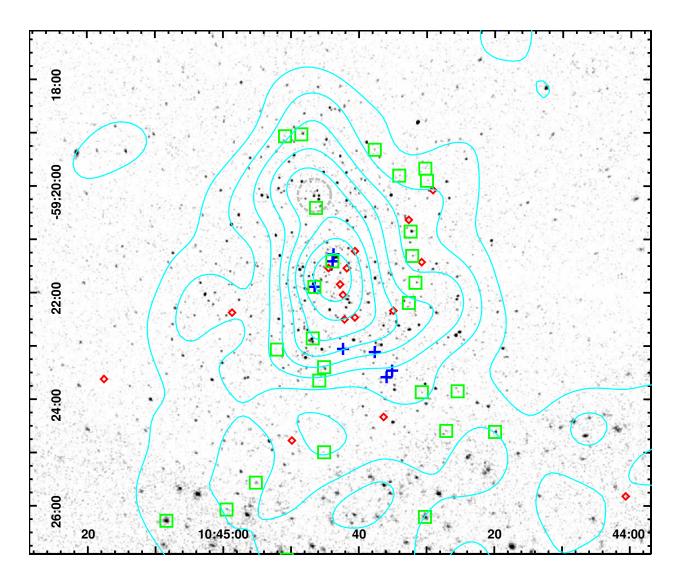
Fig. 4.— (a) Spatial distribution of three groups of stars relative to lower mass cluster members detected by the CCCP: X-ray detected (blue crosses) and undetected high mass stars (red diamonds) in Skiff (2009), and X-ray stars with K-band excess (green boxes). Density of cluster members is shown as contours (cyan) on a 0.5–7 keV X-ray image. The location of a small clump of stars noted in the text is marked with a grey circle.
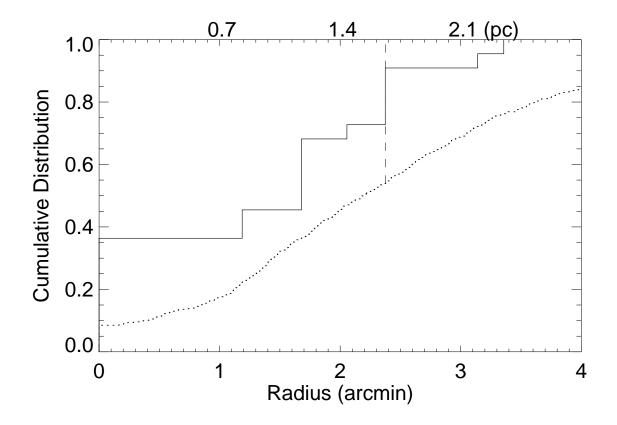
Fig. 4.— (b) One-dimensional cumulative radial distributions for all high mass stars (solid) and for the lower mass CCCP cluster members (dotted). Using a 2-sample Kolmogorov-Smirnov statistic computed at the dashed line, we find a probability of 0.4% that the two populations have the same radial profile.
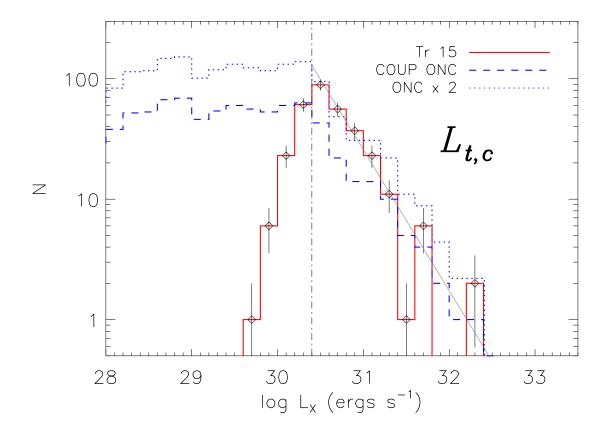
Fig. 5.— Distributions of total-band absorption corrected X-ray luminosity for 316 low-mass CCCP stars in Trumpler 15 (red solid line, 7 known OB stars omitted), and for 839 low-mass COUP stars in the ONC (blue dashed line). The blue dotted line shows the COUP XLF scaled by a factor of 2 to match Trumpler 15 for $30.4 \leq \log L_{t,c} \leq 31.0$. The grey solid line represents a fit with a power-law slope $\Gamma = -1.27$, and the vertical dash-dotted line is the estimated completeness limit for $L_{t,c}$.
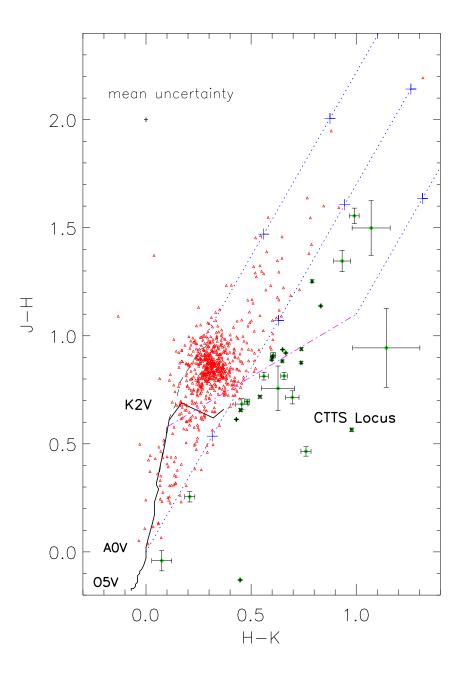
Fig. 6.— Near-IR color-color diagram ($J-H$ vs. $H-K$) for the X-ray selected Trumpler 15 probable members. The green circles and red triangles represent sources with and without significant K-band excess. The black solid and long-dash lines denote the loci of Zero Age Main Sequence (ZAMS) stars and giants, respectively, from Bessell & Brett (1988). The purple dash dotted line is the locus for classical T Tauri stars (CTTS) from Meyer et al. (1997). The blue dashed lines represent the standard reddening vector with crosses marking A_V intervals of 5 magnitudes.
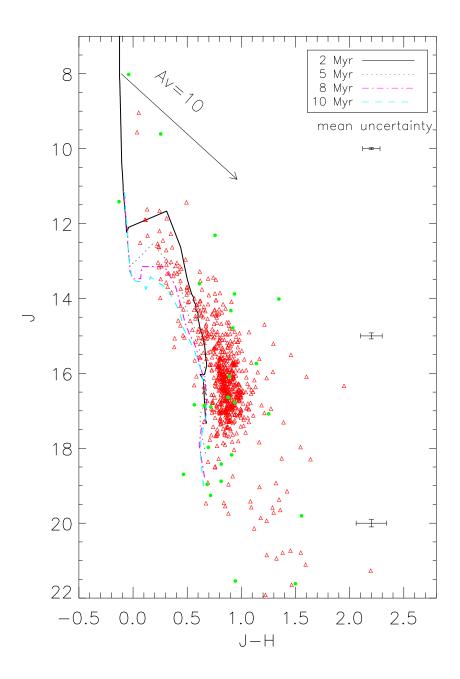
Fig. 7.— Near-IR color-magnitude diagram (J vs. $J - H$) using the same Trumpler 15 sample and symbols as in Figure 6. The solid (black) line shows the 2 Myr isochrone; the dotted (grey), the dot-dashed (magenta), and the dashed (cyan) lines show the low-mass ($M \leq 7M_\odot$) isochrones (Siess et al. 2000) for ages of 5, 8, and 10 Myr, respectively. The arrow indicates the redenning vector for $A_V = 10$ mag. Typical uncertainties of the photometry are indicated by the three error bars to the right.
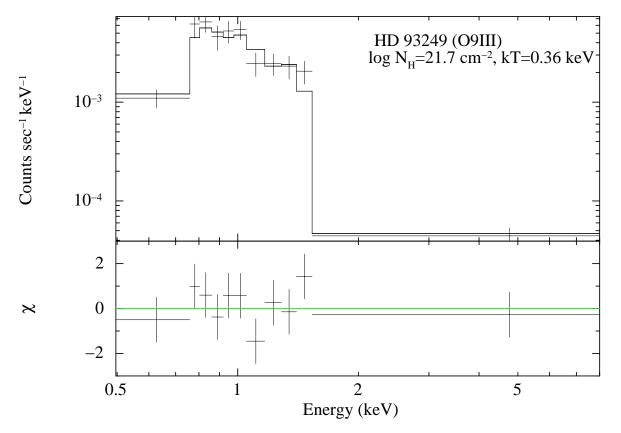
Fig. 8.— X-ray spectrum of the O9III star HD 93249 and the best fit with a simple absorbed thermal plasma model.

Table 1.   Properties of Trumpler 15 in the Literature

Reference	Distance (kpc)	Age (Myr)	Members (#))	E(B-V) (mag)
1	1.7	...	10	0.53
2	1.6	2	25	0.4
3	3.7	...	...	...
4	2.6 ± 0.2	6 ± 3	36	0.48 ± 0.07
5	2.5	...	...	0.189
6	2.4 ± 0.2	...	35	0.49 ± 0.09
7	2.4 ± 0.3	<6	90	0.52 ± 0.07
8	2.9	3-40	...	>0.42

Note. — References–[1] Grubissich (1968); [2] Thé & Vleeming (1971); [3] Walborn (1973, 1995); [4] Feinstein et al. (1980); [5] Thé et al. (1980); [6] Tapia et al. (1988); [7] Carraro (2002); [8] Tapia et al. (2003)

Table 2.   Properties of Chandra ACIS Point Sources in the Trumpler 15 Region

Seq. #	Designation (CXOGNC J)	R.A. (J2000)	Dec. (J2000))	NetCounts_t	Class
5823	104416.56-592501.3	161.069031	-59.417038	38.3	H2
5930	104418.41-592608.2	161.076736	-59.435612	12.4	H2
5968	104419.32-592209.6	161.080521	-59.369358	6.6	H2
5989	104419.66-592222.3	161.081924	-59.372875	17.6	H2
5992	104419.72-592359.4	161.082184	-59.399860	3.3	H2
6002	104419.88-592437.0	161.082840	-59.410294	30.6	H2
6023	104420.20-592534.7	161.084198	-59.426323	16.6	H2
6027	104420.25-592608.8	161.084396	-59.435799	22.1	H2
6043	104420.47-592402.2	161.085327	-59.400627	3.4	H2
6053	104420.72-592433.8	161.086365	-59.409397	2.8	H2

Note. — Table 2 with complete notes is published in its entirety in the electronic edition of the *Astrophysical Journal*. A portion is shown here for guidance regarding its form and content.

Note. — **Column 1:** CCCP X-ray catalog sequence number (Broos et al. 2011a). **Column 2:** IAU designation. **Columns 3,4:** Right ascension and declination (both in degrees) for epoch J2000.0. **Column 5:** Net X-ray events detected in the source extraction aperture in the total band (0.5–8 keV), taken from Table 1 in Broos et al. (2011a) with the identical column name. **Column 6:** A set of mutually exclusive classification hypotheses defined for each source in Broos et al. (2011b)—H0: source is unclassified; H1: source is a foreground main-sequence star; H2: source is a young star, assumed to be in the Carina complex; H3: source is a Galactic background main-sequence star; H4: source is

extragalactic.

Note. — Notes/other names from SIMBAD queries using a $2''$ matching radius:

[6860]—Cl Trumpler 15 20=GSC 08626-00886=GEN# +4.35150020

[6907]—Cl Trumpler 15 19=Cl* Trumpler 15 C 28=GEN# +4.35150019

[7023]—Cl Trumpler 15 21=Cl* Trumpler 15 C 44=GEN# +4.35150021

[7195]—Cl Trumpler 15 8=GSC 08626-01516=GEN# +4.35150008

[7318]—Cl Trumpler 15 15=CPD-58 2656=Cl* Trumpler 15 C 3= GSC 08626-01303=GEN# +4.35150015=TYC 8626-1303-1

[7332]—Cl Trumpler 15 6=NSV 18508

[7397]—Cl Trumpler 15 2=CCDM J10447-5921B=Cl* Trumpler 15 C 2=GSC 08626-02845=GEN# +4.35150002

[7403]—Cl Trumpler 15 1=HD 93249=ALS 1857=1E 1042.7-5905=SAO 238421=CCDM J10447-5921A=GEN# +4.35150001J

[7584]—Cl Trumpler 15 10=Cl* Trumpler 15 C 17 =CPD-58 2662= GSC 08626-01107 =GEN# +4.35150010

[7679]—Cl Trumpler 15 12=GSC 08626-01694 = GEN# +4.35150012

[7696]—Cl Trumpler 15 38 = GEN# +4.35150038=2MASS J10444861-5922153

[7756]—Cl Trumpler 15 29 = GSC 08626-01760 = GEN# +4.35150029

[8235]—Cl Trumpler 15 31 = GEN# +4.35150031

[8503]—Cl Trumpler 15 35 = GEN# +4.35150035=2MASS J10450167-5923382

[8554]—Cl Trumpler 15 34 = GEN# +4.35150034=2MASS J10450269-5922019

Table 3.   CCCP Detected OB Stars in the Trumpler 15 Region

Name Cl Trumpler 15	CCCP ID	R.A. (J2000)	Dec. (J2000))	Sp.Type	V (mag)	X-ray Cts (0.5–8 keV)	Note
1	7403	161.18283	-59.35700	O9III	8.40	184	HD 93249; CD-58 3536
2	7397	161.18229	-59.35481	O9.5:III	9.50	17	CD-58 3536B
10	7584	161.19387	-59.36497	B2V	11.60	7	CPD-58 2662
15	7318	161.17642	-59.38439	B0.5IV-V	10.10	14	CPD-58 2656
19	6907	161.14967	-59.39322	O9:V:	12.70	12	...
20	6860	161.14629	-59.39117	O9 V:	12.70	3	...
21	7023	161.15692	-59.38536	B0:III:	13.10	3	...

Note. — **Column 1:** Name of Trumpler 15 OB stars originally defined by Grubissich (1968). **Column 2:** CCCP X-ray catalog sequence number (Broos et al. 2011a). **Columns 3,4:** Right ascension and declination (both in degrees) for epoch J2000.0. **Column 5:** Spectral type as classified in Skiff (2009). **Column 6:** V magnitude (Carraro 2002). **Column 7:** Net X-ray events detected in the source extraction aperture in the total band (0.5–8 keV), taken from Table 1 in Broos et al. (2011a) with column name "NetCounts_t". **Column 8:** Other designations listed in SIMBAD.